World Academy of Science, Engineering and Technology
International Journal of Electronics and Communication Engineering
Vol:16, No:4, 2022

Spatial Correlation of Channel State Information in Real LoRa Measurement

Ahmed Abdelghany, Bernard Uguen, Christophe Moy, Dominique Lemur

Abstract—The Internet of Things (IoT) is developed to ensure monitoring and connectivity within different applications. Thus, it is critical to study the channel propagation characteristics in Low Power Wide Area Network (LPWAN), especially LoRaWAN. In this paper, an in-depth investigation of the reciprocity between the uplink and downlink Channel State Information (CSI) is done by performing an outdoor measurement campaign in the area of Campus Beaulieu in Rennes. At each different location, the CSI reciprocity is quantified using the Pearson Correlation Coefficient (PCC) which shows a very high linear correlation between the uplink and downlink CSI. This reciprocity feature could be utilized for the physical layer security between the node and the gateway. On the other hand, most of the CSI shapes from different locations are highly uncorrelated with each other. Hence, it can be anticipated that this could achieve significant localization gain by utilizing the frequency hopping in the LoRa systems to get access to a wider band.

Keywords—IoT, LPWAN, LoRa, RSSI, effective signal power, onsite measurement, smart city, channel reciprocity

I. Introduction

INTERNET of Things (IoT) has been employed in a wide range of domains, such as security, industrial monitoring, smart homes, smart cities, smart agriculture, etc [1]. These applications require a large coverage network, low power consumption, and a cheap deployment. Hence, Low Power Wide Area Network (LPWAN) is considered a leading technology for achieving this requirement, especially the LoRaWAN [2]. This ability is manifested in the LoRaWAN design which compromises between a large communication range and low energy consumption [3].

Recently, different characteristics of LoRa propagation are mentioned in many works. For example, the physical and data link layer performance is evaluated by field tests and simulations in [4] while the coverage and channel attenuation of LoRa technology are evaluated for real environments in [5] and [6]. In [7], path loss models are developed and compared with widely used empirical models based on empirical results. On the other hand, the feasibility of utilizing the Channel State Information (CSI) for localization is studied in [3]. However, these previous works do not investigate the spatial correlation of CSI, or even the reciprocity between the uplink and downlink CSI that could be exploited in some security procedures in the LoRaWAN [8].

In this paper, a real network deployment is employed to investigate the CSI shapes at various locations within the area of the Campus Beaulieu in Rennes. Hence, the Effective Signal Power (ESP) is used for this investigation to overcome the limitation of the RSSI at low SNR ($< 0\,\mathrm{dB}$), as proven in [9]. Thus, ESP values are average at each frequency band to estimate the absolute CSI of the uplink and downlink transmission. Consequently, the CSI reciprocity, as well as the spatial evolution of the CSI, are analyzed using the Pearson Correlation Coefficient (PCC).

The remainder of this paper is organized as follows. Section II presents the measurement overview. Section III provides sufficient detail about the estimation of the CSI shape. The reciprocity between uplink and downlink CSI is then investigated in Section IV. Then, Section V provides an evaluation of the spatial correlation between the CSI shapes. Finally, the work is concluded in Section VI.

Ahmed Abdelghany, Bernard Uguen, Christophe Moy, and Dominique Lemur are with Univ Rennes, CNRS, IETR - UMR 6164, F-35000, Rennes, France (e-mail: ahmed.abdelghany, bernard.uguen, christophe.moy, dominique.lemur@univ-rennes1.fr).

II. Measurement Overview

The main aim of the proposed experiment is to obtain the average ESP value at each frequency band. This is achieved by placing an IoT node at various distances in the range of $\approx 5\,\mathrm{m}$ to $\approx 800\,\mathrm{m}$, as shown in Fig. 1 while the LoRaWAN Configuration is set as depicted in Table I. At the typical frequency bands for Europe, i.e. 8 channels with center frequency f_k, confirmed LoRa packets are transmitted sequentially with $125\,\mathrm{kHz}$ bandwidth W.

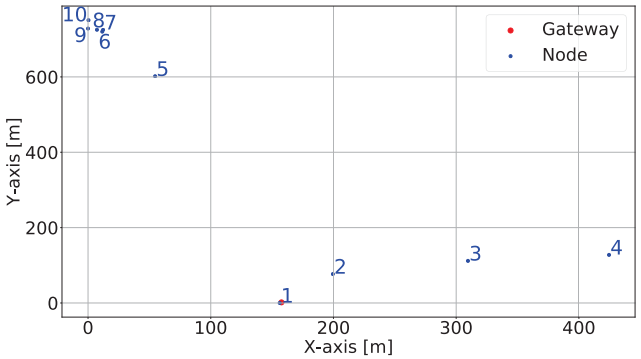

Fig. 1 The topology of the end node locations within the area of the Campus Beaulieu

A Tektelic KONA Macro Gateway, whose antenna is fixed on the roof of the university building, is used in this experiment [10], as shown in Fig. 2a. The end node is implemented using a Pycom card, i.e. programmed in the MicroPython language, composed of an Expansion Board and a LoPy 4 module which can support LoRa wireless connectivity [11], as shown in Fig. 2b. This Pycom node

TABLE I
LoRaWAN Configuration

LoRaWAN Parameter	Value
Modulation technique	LoRa (based on CSS)
Spreading Factor (SF)	7
Coding rate	4/5
Bandwidth W	125 kHz
Transmit power	14 dBm
Center frequency f_k	$\{867.1, 867.3, 867.5, 867.7, 867.9, 868.1, 868.3, 868.5\}$ MHz

transmits an uplink packet for each specific channel f_k while the gateway attempts to send an acknowledgment by default at the same frequency as the message transmitted. Accordingly, the node writes the information of the last received downlink packet (packet number, ESP, etc.) to the payload of the next uplink packet. A desktop computer-run a Python program is used as an Application Server (AS) which receives data from the LoRa Network Server (LNS), as well as LoRa metadata with all parameters of the LoRaWAN transmission (f_k, SF, Bandwidth W, RSSI, SNR, etc.). Consequently, the computer stores this data for processing as detailed in the following sections. For the research society, the data are provided on this online repository [12].

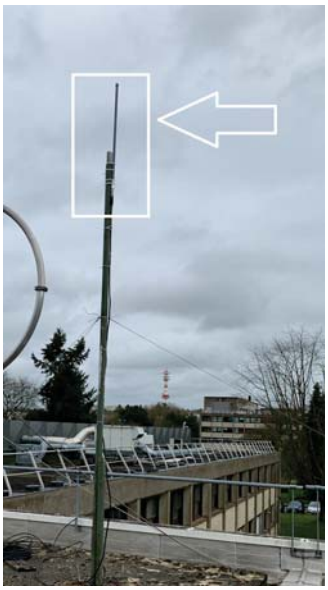

(a) The gateway monopole antenna connected to the cable

(b) The packaged Pycom device fixed on a rod and connected to a battery at location 4.

Fig. 2 Views from the end node and gateway sites.

III. CSI Shape Estimation

On the gateway side, the received data are extracted from the payload of each received packet plus the metadata. Without loss of generality, ESP is proven in [9] to be more reliable than the RSSI which has a limitation when the SNR is very low. For this, ESP is estimated as:

$$ESP_{dBm} = RSSI_{dBm} + SNR_{dB} - 10\log_{10}(1+10^{0.1SNR_{dB}}). \quad (1)$$

As an approach for obtaining the absolute CSI, uplink ESP, uplink and downlink ESP values are averaged at each frequency channel f_k. As an example shown in Fig. 3a, the absolute CSI from location 2 is frequency selective with a deep fade of more than 15 dB depth, particularly at 867.5 MHz. Moreover, channel reciprocity is manifested between the uplink and downlink CSI with almost the same fading position. While in Fig. 3b, the obtained CSI also indicates multipath propagation whose deep fades are up to 10 dB depth. Apart from a constant value whose compensation would require an accurate calibration of the transceiver RF chains, the same channel reciprocity across all the frequency bands is preserved. On the other hand, one can observe that the gap between the uplink RSSI and ESP is larger in Fig. 3b than in Fig. 3a, as indicated by the black arrows. This behavior is clarified by (1), thus, the gap between the RSSI and ESP increases when SNR decreases below 0 dB. Therefore, the RSSI values are ignored, whereas the ESP values are utilized for further investigations as detailed in the following sections.

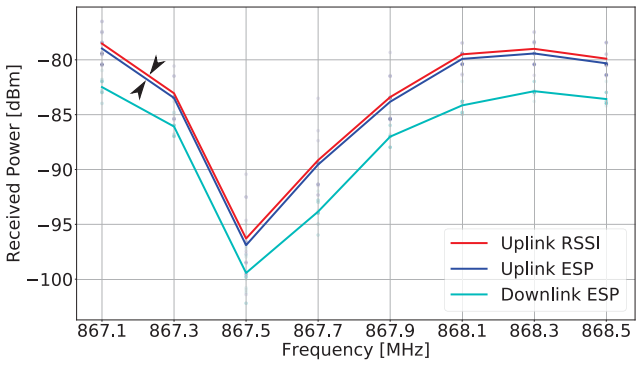

(a) The absolute CSI from location 2

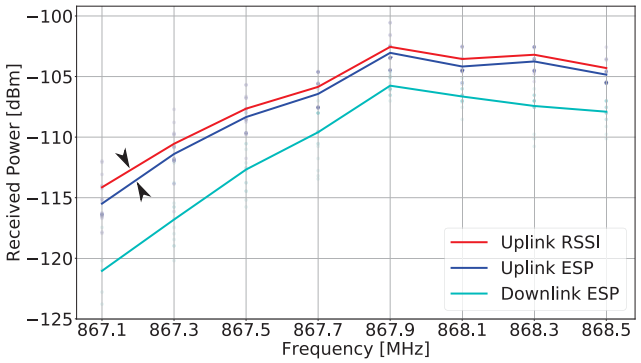

(b) The absolute CSI from location 7

Fig. 3 The absolute CSI shape from different locations

IV. Reciprocity of the CSI Shapes

In this section, the magnitude of the aforementioned CSI reciprocity is evaluated for all the locations. To quantitatively appreciate the similarity or dissimilarity of the frequency dependency of quantities, for example, the uplink versus downlink ESP values, PCC is utilized [13].

Let:

$$\mathbf{x} = [x_0, \ldots, x_{N-1}]^T \tag{2}$$

and

$$\mathbf{y} = [y_0, \ldots, y_{N-1}]^T \tag{3}$$

be two frequency dependent vectors of the same size N, where N in this experiment corresponds to the number of the frequency channels f_k. Consequently, the centered versions of those two vectors are:

$$\mathbf{x_c} = \mathbf{x} - \frac{\mathbf{x}^T.\mathbf{1}_N}{N} = \mathbf{x} - \bar{\mathbf{x}} \tag{4}$$

and

$$\mathbf{y_c} = \mathbf{y} - \frac{\mathbf{y}^T.\mathbf{1}_N}{N} = \mathbf{y} - \bar{\mathbf{y}}. \tag{5}$$

At this point, the PCC between those two vectors is classically expressed as a simple dot product between their normalized versions as:

$$\rho_{xy} = \hat{\mathbf{x}}_\mathbf{c}^T.\hat{\mathbf{y}}_\mathbf{c} = \frac{{\mathbf{x_c}}^T.\mathbf{y_c}}{\sqrt{{\mathbf{x_c}}^T\mathbf{x_c}}\sqrt{{\mathbf{y_c}}^T\mathbf{y_c}}}. \tag{6}$$

This correlation coefficient is a measure of the linear correlation between those two vectors which captures only their fluctuations around their centers. Hence, this coefficient is essentially a normalized value, such that the result always has a value between -1 and 1.

By utilizing the PCC for quantifying the reciprocity of the uplink versus downlink CSI, Fig. 4 shows the magnitudes of the PCC across all the locations. The result shows that most of the PCC values are greater than 0.9 which represents a nearly identical shape of CSI between the uplink and downlink transmission. For future IoT applications, this reciprocity feature could be exploited for the physical layer security between the node and the gateway [8]. However, locations 3 and 10 have the lowest PCC values due to the lack of the averaged ESP values at some frequency bands, hence, this often happens as a reason for the packet transmission losses.

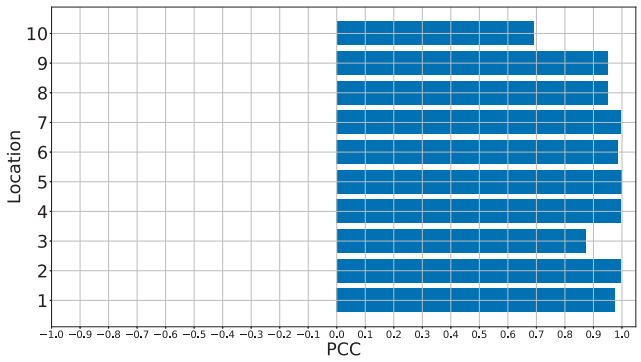

Fig. 4 The PCC magnitude between the uplink and downlink CSI at each location

V. Spatial Correlation of the CSI Shapes

For investigating the spatial correlation between the CSI shapes from different positions, the CSI spatial evolution between each location combination i and j is analyzed using the aforementioned method, which is based on the PCC. As depicted in Fig. 5a, most of the PCC magnitudes are generally unrelated to the Euclidean distance at any two locations in Fig. 5b. In contrary to the nearly similar uplink and downlink CSI which is demonstrated by the high reciprocity for a single stationary location, hence, the CSI shape is varying from one place to another even for short separations. This behavior is reasonable as the minimum Euclidean distance between any two locations is $\approx 4.9\,\mathrm{m}$ in this experiment. This suggests the feasibility of utilizing the CSI for localization provided that this CSI remains stationary enough over time. Based on that, the accuracy of positioning could be improved by utilizing the rich channel information in each subcarrier f_k, thanks to the frequency hopping in the LoRa systems. Hence, the individual CSI shape from each different location has to be appropriately different from one another to achieve significant localization gain.

VI. Conclusion

This paper investigates the reciprocity between the uplink and downlink CSI in LoRa, moreover, the spatial evolution of the CSI from different locations is analyzed. Accordingly, a measurement campaign is carried out in the city of Rennes to estimate the CSI by averaging ESP values at each frequency band. For that, ESP is utilized to obtain the CSI shape since it is more reliable than RSSI, as it overcomes the RSSI limitation, especially at low SNR ($< 0\,\mathrm{dB}$). On the other hand, PCC is utilized to quantify the linear correlation between two CSI shapes. As a result, the estimated uplink and downlink CSI shapes are almost analogous at most of the node locations. Furthermore, the CSI shapes from different locations are highly uncorrelated with each other.

For future work, this paper recommends using this reciprocity feature for the physical layer security between the end node and the gateway. Moreover, the unique CSI shape at each location could achieve significant localization gain by utilizing the frequency hopping in the LoRa systems to get the rich channel information in each subcarrier.

Acknowledgment

We are grateful to Jean François Legendre from Gwagenn Company for lending us the gateway [14].

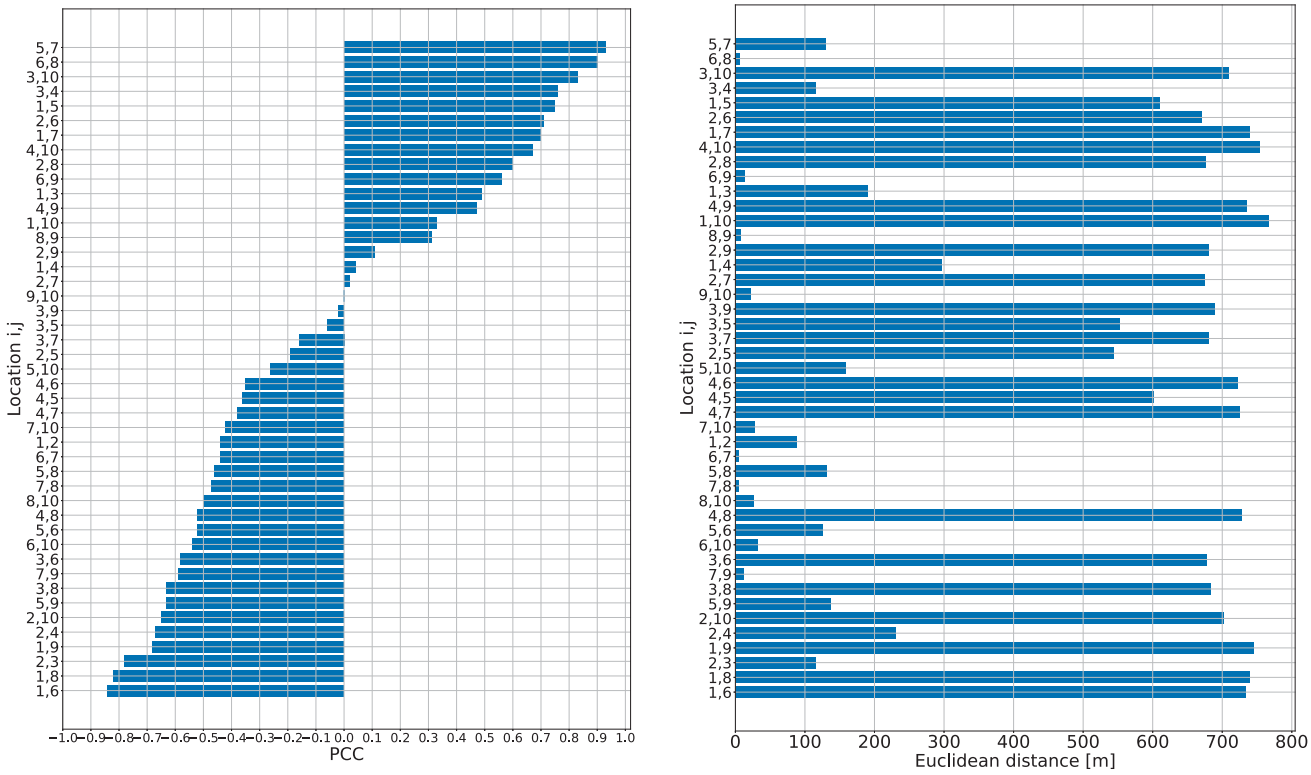

(a) PCC values

(b) Euclidean distance values

Fig. 5 PCC and Euclidean distance values across all the location combinations

REFERENCES

[1] A. A. Ghany, B. Uguen and D. Lemur, "A Pre-processing Algorithm Utilizing a Paired CRLB for TDoA Based IoT Positioning," 2020 IEEE 91st Vehicular Technology Conference (VTC2020-Spring), Antwerp, Belgium, 2020, pp. 1-5, doi: 10.1109/VTC2020-Spring48590.2020.9128385.

[2] LoRa-Alliance - https://www.lora-alliance.org/

[3] A. A. Ghany, B. Uguen and D. Lemur, "A Robustness Comparison of Measured Narrowband CSI vs RSSI for IoT Localization," 2020 IEEE 92nd Vehicular Technology Conference (VTC2020-Fall), 2020, pp. 1-5, doi: 10.1109/VTC2020-Fall49728.2020.9348854.

[4] Augustin, A.; Yi, J.; Clausen, T.; Townsley, W.M. A Study of LoRa: Long Range & Low Power Networks for the Internet of Things. Sensors 2016, 16, 1466.

[5] L. Li, J. Ren and Q. Zhu, "On the application of LoRa LPWAN technology in Sailing Monitoring System," 2017 13th Annual Conference on Wireless On-demand Network Systems and Services (WONS), Jackson, WY, 2017, pp. 77-80, doi: 10.1109/WONS.2017.7888762.

[6] M. R. Seye, B. Ngom, B. Gueye and M. Diallo, "A Study of LoRa Coverage: Range Evaluation and Channel Attenuation Model," 2018 1st International Conference on Smart Cities and Communities (SCCIC), Ouagadougou, 2018, pp. 1-4, doi: 10.1109/SCCIC.2018.8584548.

[7] R. El Chall, S. Lahoud and M. El Helou, "LoRaWAN Network: Radio Propagation Models and Performance Evaluation in Various Environments in Lebanon," in IEEE Internet of Things Journal, vol. 6, no. 2, pp. 2366-2378, April 2019, doi: 10.1109/JIOT.2019.2906838.

[8] M. Bloch, J. Barros, M. R. D. Rodrigues and S. W. McLaughlin, "Wireless Information-Theoretic Security," in IEEE Transactions on Information Theory, vol. 54, no. 6, pp. 2515-2534, June 2008, doi: 10.1109/TIT.2008.921908.

[9] Ahmed Abdelghany, Bernard Uguen, Christophe Moy, Dominique Lemur. On Superior Reliability of Effective Signal Power versus RSSI in LoRaWAN. 28th International Conference on Telecommunications (ICT 2021), Jun 2021, London, United Kingdom. (hal-03210318)

[10] Tektelic KONA Macro IoT Gateway. https://www.tektelic.com/uploads/Brochures/Kona\%20Macro.pdf

[11] Pycom documentation: https://GitHub.com/PyCom/PyCom-libraries

[12] Measurement Data. https://gitlab.com/ahmednagy/lorawan-beaulieu-measurement-2020

[13] Benesty J., Chen J., Huang Y., Cohen I. (2009) Pearson Correlation Coefficient. In: Noise Reduction in Speech Processing. Springer Topics in Signal Processing, vol 2. Springer, Berlin, Heidelberg. https://doi.org/10.1007/978-3-642-00296-0-5

[14] Gwagenn company website.http://www.gwagenn.com/en/home/